

## Modelling and Interpretation of Condensate Banking for the Near Critical Cupiagua Field

Sheng-Tai Lee, BPX Houston, TX, and Marcial Chaverra, BPX-Colombia (Bogota-Colombia)

Copyright 1998, Society of Petroleum Engineers, Inc.

This paper was prepared for presentation at the 1998 SPE Annual Technical Conference and Exhibition held in New Orleans, Louisiana, 27-30 September 1998.

This paper was selected for presentation by an SPE Program Committee following review of information contained in an abstract submitted by the author(s). Contents of the paper, as presented, have not been reviewed by the Society of Petroleum Engineers and are subject to correction by the author(s). The material, as presented, does not necessarily reflect any position of the Society of Petroleum Engineers, its officers, or members. Papers presented at SPE meetings are subject to publication review by Editorial Committees of the Society of Petroleum Engineers. Electronic reproduction, distribution, or storage of any part of this paper for commercial purposes without the written consent of the Society of Petroleum Engineers is prohibited. Permission to reproduce in print is restricted to an abstract of not more than 300 words; illustrations may not be copied. The abstract must contain conspicuous acknowledgment of where and by whom the paper was presented. Write Librarian, SPE, P.O. Box 833836, Richardson, TX 75083-3836, U.S.A., fax 01-972-952-9435.

### Abstract

Near-well condensate banking has been recognized as a main factor causing deliverability loss of condensate wells. The problem is particularly acute for low-permeability high-yield condensate systems. The very high-yield nature of the hydrocarbons leads to a significant condensate dropout once the reservoir pressure becomes lower than the original dew point pressure. The low-permeability rocks, in turn, cause significant pressure drops, exacerbating condensate banking.

This paper presents a fundamental study on the mechanisms controlling deliverability of low-permeability condensate wells in the giant, near-critical Cupiagua field in Colombia. The study combines results from three areas of work, namely (i) interpretation of long-term (approximately six months) well production and build-up test data for three appraisal wells, (ii) fine-grid radial single-well equation-of-state compositional modelling of the long-term well test and (iii) rigorous application and validation of the single-well pseudo-steady-state-flow theory to predicting production rates of condensate wells.

First, we present compositional modelling work to history match the production test data (e.g. GOR and production rates versus time) for three rich-condensate wells. The history-matched compositional model is then used to analyze the in-situ phase behavior and condensate banking phenomena during production. The analysis of model results provides a clear understanding on the key factors which control well deliverability. Particularly, we have found that in-situ condensate re-vaporization is directly related to increase of production GOR and loss of deliverability. The factors which affect re-

vaporization are then investigated through the compositional model.

The well-known pseudo-steady-state theory for flow of single-well condensate wells is then re-examined with the aim of using the simple pseudo-steady-state formulation to calculate the deliverability of condensate wells. It is demonstrated that the in-situ phase behavior and PVT properties calculated by the pseudo-steady-state model match closely those from a general EOS compositional model. Further, the pseudo-steady-state model is shown to be applicable beyond the infinitely-acting-reservoir flow period, within which the GOR is constant. Application of the pseudo-steady-state model is demonstrated using a set of field-measured production data.

### Introduction

Well deliverability is an important subject for appraisal and development of condensate field. It is a critical parameter which provides forecasts of production and well requirement. The well deliverability is also needed for designing facility and for determining overall economics of field development.

During early development of the near-critical Cupiagua field, condensate banking and tight formation rock have been recognized as important factors which could affect long-term well deliverability. Extensive studies have been carried out through laboratory fluid PVT experiments, reservoir condition core floods, partial and full-field compositional modelling to understand the Cupiagua subsurface process mechanisms and to optimize the field development. The work on well deliverability presented in this paper is part of the on-going Cupiagua subsurface activities at BP Exploration-Colombia, which operates the Cupiagua field.

Accurate prediction of long-term well deliverability can be attained via a rigorous compositional modelling approach involving a good description of reservoir rock parameters, an accurate equation of state (EOS) for the reservoir fluid and an adequate near wellbore mechanistic model within the simulator. The near-wellbore model would include non-Darcy effects and viscous force enhanced condensate mobility<sup>1,2</sup>

One much simpler alternative to compositional modelling for well deliverability is the use of pseudo-pressure function to represent the pressure drop across the flowing bottomhole into

the reservoir. This approach involves the assumption of a steady state flow condition within the reservoir at any time during production. Such an approximation significantly simplifies the governing flow equations, while simultaneously captures the essential physics involved. This approach appeared to have been first used by O'Dell and Miller<sup>3</sup> for a low-permeability and high-yield condensate reservoir. The concept has since been adopted and tested by several authors<sup>4,5,6</sup> for calculating condensate well deliverability. Particularly notable is the work by Fevang and Whitson who formally formulated the three flow regimes during condensate banking in terms of steady-state pseudo-pressure functions and emphasized the important requirement of production GOR for the pseudo-steady state model.

The main objective of this work is to develop a capability of forecasting well deliverability for the Cupiagua field. This capability could be achieved through rigorous compositional modelling and validation of model results with available field data. Further, the validated compositional model is then used to evaluate the pseudo-steady-state model for routine calculations of well deliverability.

In this paper, we first present a brief description of the main PVT properties of the Cupiagua field. Then, we discuss one-D compositional modelling to match the production data from three appraisal wells. The compositional model provides a basis for understanding the mechanisms and factors, which control the well production during depletion. The pseudo-steady-state model was then reviewed. The production GOR is deemed a key measurable parameter, which mechanistically signals the production efficiency and serves as input to the pseudo-steady-state model. The factors which control the production GOR increase was investigated using the compositional model. Finally, the pseudo-steady-state-model was evaluated by comparing with the EOS compositional model in terms of predicted in-situ PVT properties, and with field-measured gas production data.

### The Field and the Hydrocarbon System

The giant Cupiagua field lies in the deep Colombian Foothills Belts of the Llanos Basin in Colombia. The true vertical depths for the hydrocarbon reservoirs are typically beyond 10,750 ft sub-sea with in-situ pressures and temperatures higher than about 6200 psi and 240°F, respectively. The hydrocarbon column covers a seemingly communicating vertical thickness of about 5000 feet, within which the reservoir temperature increases from 240°F at the crest to about 300°F near the hydrocarbon-water contact. The combined geologic and thermodynamic conditions (i.e. deep, high temperature and high pressure, hydrocarbon sources and a continuous hydrocarbon column) imply complex reservoir fluid phase behavior and PVT properties. Indeed, most of the hydrocarbons exist as a near critical condensate system with an average surface condensate yield of 300 stb/mm scf and condensate API gravity of about 42-43°.

Figures 1 and 2 highlight the main characteristics of the hydrocarbon system. Figure 1 shows the original reservoir

pressure and fluid saturation pressure versus vertical depth and reservoir temperature. The dew-point pressure distribution versus depth was calculated through an EOS, along with a compositional extrapolation methodology<sup>7</sup>. The EOS-predicted PVT properties (including dew point pressure) were validated with 10 fluid samples which were collected during a two-year period. It shows that the hydrocarbon dew-point pressure changes rather mildly in the range of 5300 to 5350 psia within a vertical distance of 5000 feet. The increasing reservoir pressure with depth then makes the fluid increasingly undersaturated down-dip. Figure 2 is a pressure-temperature phase diagram for a fluid sampled at 12,300 fss TVD interval. It is shown that the in-situ hydrocarbon system is close to a thermodynamic critical condition, and when depleted below the dew point pressure a significant liquid condensate (40-45% HCPV) will drop out for most pressure conditions. Based on observation from laboratory experiment (opalescence, phase-volume relationship, etc.) the fluid system remains at a near critical condition for pressures down to about 4000 psi. There were several measured IFT data for the Cupiagua hydrocarbon systems; for example, at 255°F and 5000 psia, the IFT was measured to be about 0.01 dyne/cm<sup>8</sup>.

### One-D Single-Well Compositional Modelling and Matching of Production Data

For a period of about two years, long-term production fluid production data were obtained from three appraisal wells, designated as Wells A, B and C. To understand the single-well production mechanisms and to later validate the pseudo-steady-state model, a one-D radial single-well compositional model was developed.

Our compositional model uses the commercial VIP Reservoir Simulator by Landmark. The model consisted of 100 radial grid-blocks with uniform rock properties. The grid-block sizes are non-uniform, with a logarithmic progression toward radial reservoir boundary; the ten inner-most grid-blocks have thickness ranging from 1 to 2 feet. Basic model input data for reservoir and near-well flow properties were determined from petrophysical core data and well test<sup>14</sup> during early production. Table 1 lists certain model parameters of interest.

The compositional model takes into account the effect of the near well non-Darcy turbulence effect. The "turbulence" factors used were determined through well testing<sup>14</sup>. A single set of relative permeability curves was used for the three well. Effect of near-critical low interfacial tension on relative permeability was accounted for in a conventional manner. A critical condensate saturation of 32% PV was used in the model.

A single EOS, along with a field-wide compositional table, was used to initialize the hydrocarbon system for each well. In accordance with surface production operation, the model set tubing head pressure equal to 1200 psi for all times and used wellbore hydraulics to calculate the flowing bottomhole pressures (FBHP) and the production rates. Table 2 lists the original reservoir and fluid dew-point pressures and tempera-

tures for the three wells.

During the one-D modelling and matching of available production data, it was thought that the production GOR is an important measured parameter which indicates the production efficiency of the well. The production GOR, in addition, is a required input parameter in the pseudo-steady-state model, which will be discussed later. At the time of the work, there was uncertainty about the size of drainage area covered by each testing well. The drainage radius, used in the model, affects critically the production GOR behavior. As a result, it was decided to express the model-predicted GOR directly in terms of the cumulative gas production (CGP), and compare the results with field-measured counterparts.

**Figure 3** compares the model-predicted GOR in terms of CGP versus the field measured data for the three wells. It is shown that the compositional model is capable of correlating accurately the GOR behavior versus CGP. From the good match, we identified two important parameters which affect the observed GOR behavior among the three wells; these are the degree of fluid undersaturation (**Table 2**) and the drainage radius used in each well. Both factors are related to reservoir energy to sustain a single-phase system and to impede two-phase propagation.

**Figure 4** compares the model-calculated GOR versus measured data during a pressure build-up test, which occurred after the well had been on production for two month. It is shown that the model-predicted GOR is consistent with the data, in that a higher shut-in pressure lowers the production GOR.

The good accuracy of the compositional model with respect to field production data lends confidence to using the model to investigate process mechanisms (particularly with respect to factors controlling GOR increase), and to examine validity of the pseudo-steady-state model. Both subjects will be presented later. For completeness, a brief discussion on the formulation of pseudo-steady-state model is made in the following section.

**Review and Discussion of Pseudo-Steady-State Model**

The delineation of flow regime by phase behavior occurred during depletion of condensate reservoirs has been discussed in the literature.<sup>5,6,9,10</sup> For discussion, we follow the description by Fevang and Whitson, who denoted the possible flow regimes by

Region 1: occurring nearest to the producing well, where there are two flowing hydrocarbon phases (gas and condensate);

Region 2: containing only one flowing phase (gas) and with a condensate saturation less than its critical value; and

Region 3: containing only one phase (gas), with regional pressure greater than the original dew point pressure.

Depending on pressure and fluid phase behavior, one or two regions could disappear. The definition of the three flow regions is consistent with physics and can be analyzed through the pseudo-steady-state model. **Figure 5** summarizes the main

characteristics of the three regions.

The general volumetric gas production rate for a condensate well without non-Darcy effect can be expressed through the conventional pseudo-pressure function as<sup>4,5,6</sup>

$$q_g = A \cdot \frac{m(P_r) - m(P_{bh})}{\ln(r_e / r_w) - 0.75 + S} \dots\dots\dots(1)$$

where the parameter  $A = \frac{KH}{141.2} \left( \frac{RT_s}{P_s} \right) \cdot \beta_s$

and the psuedo-pressure function can be calculated as

$$m(P_r) - m(P_{bh}) = \int_{P_{bh}}^{P_r} \left( \frac{\rho_o k_{ro}}{M_o \mu_o} + \frac{\rho_g k_{rg}}{M_g \mu_g} \right) dp \dots\dots\dots(2)$$

The formulation with non-Darcy effect near the wellbore will be presented later in this section.

It is important to notice that the integration for the pseudo-pressure is carried out with respect to pressure. Further, the relative permeability ratio, related to the integrand functions in Equation (2), can be expressed as

$$\frac{k_{rg}}{k_{ro}} = \frac{q_g}{q_o} \cdot \frac{\mu_r}{\mu_o} = \frac{S_g}{S_o} \cdot \frac{\mu_r}{\mu_o} = f(T, P, x_i, y_i; z_i) \dots\dots\dots(3)$$

where  $q_g$  and  $q_o$  are the volumetric flow rates of gas and oil (within the hydrocarbon stream), and  $z_i$  is the overall *flowing* hydrocarbon component mole fraction,  $S_o$  and  $S_g$  are the flowing condensate and gas saturations in the *flowing* hydrocarbon stream (Region 1).

In other words, according to Equation (3), if the pseudo-steady-state assumption holds, then the relative permeability ratio and the flowing hydrocarbon fractions are purely thermodynamic properties, dependent only on the local pressure and the total composition  $z_i$ , which is a constant throughout the flowing regions. In particular, for Region 1, where there are two flowing phases,  $q_g/q_o$  is the same as  $S_o/S_g$  obtained from a constant-composition-expansion to the local pressure using  $z_i$  as the original composition. With thermodynamic information from an EOS, the pseudo-pressure integration of Equation (2) can be carried out numerically.

From the equations and discussion above, it can be recognized that the pseudo-steady-state model requires three key input parameters, related to reservoir fluids; these are:

1. The flowing bottomhole pressure ( $P_{bh}$ )-the lower bound of the integration in Equation (2): In general,  $P_{bh}$  is constrained by the tubing head pressure. In our compositional modelling work, a wellbore hydraulics package is used in connection with the compositional model to calculate  $P_{bh}$  during depletion. The  $P_{bh}$  value, however, must be available in the pseudo-steady-state model.
2. The average reservoir pressure ( $P_r$ )-the upper bound of the integration in Equation (2): The  $P_r$  value are general determined through material balance, given a value of drainage radius.
3. Most importantly, the flowing composition,  $z_i^*$  at a

given time of interest.

The flowing compositions,  $z_i^*$ , is equivalent to the production GOR measured at surface. As pointed out by Fevang and Whitson, the production GOR (or  $z_i^*$ ) is the key of the pseudo-steady-state model. In field production situation, the production GOR can be measured, and the increase of GOR would signal reduction of well productivity. An important subject of forecasting well deliverability is to be able to predict the GOR trend during production.

Assuming now that the production GOR is known from field production or from a compositional model, then we can calculate mathematically the flowing composition ( $z_i^*$ ), corresponding to this GOR. Using a good EOS, the dew-point pressure at reservoir temperature for the GOR can be calculated; this dew-point pressure is designated as  $P^*$ . Based on the values of  $P^*$  versus the original dew-point pressure (designate as  $P_{dew}$ ), we can have three conditions of flow regimes which are important when calculating the integration in Equation (2); these are in time sequence:

1.  $P^* = P_{dew} < P_i$ , or equivalently the production GOR is equal to the original GOR and  $z_i^*$  equal to the original composition: The flow is under an infinitely acting condition (a true steady-state, stabilized flow, period). Such a flow condition occurs the earliest after a well is put on production. Since the flowing composition is the original one, and  $P^* = P_{dew}$ , Region 2 cannot exist. Yet if  $P_{bh} < P_{dew}$  Region 1, which has two-flowing hydrocarbon phases, will exist. In general, therefore, Region 1 occurs earlier than Region 2. Furthermore, with Region 2 being absent, the condensate saturation profile should exhibit a sharp discontinuity from zero to the critical condensate saturation when the reservoir pressure drop below the original dew point pressure. This observation can be used for testing numerical accuracy of a compositional model as well as accuracy of a pseudo-steady-state model.
2.  $P^* < P_{dew} < P_e$ , or production GOR larger than the original GOR: the three flow regions could co-exist simultaneously. Based on cases studied in this work, the time period covering such a flow condition is relatively short.
3.  $P^* > P_e$  and production GOR is larger than the original GOR: The entire reservoir has been depleted and two flowing hydrocarbon phases prevail through out the reservoir.

For the case with near-wellbore non-Darcy effect, the gas rate,  $q_g$ , becomes quadratic with respect to the pseudo-pressure function, i.e.

$$m(P_r) - m(P_{bh}) = \frac{q_g}{A} \left[ (\ln(r_c / r_w) - 0.75 + S) + D \cdot q_g \right] \dots\dots\dots (4)$$

where constant  $A$  is defined with Equation (1), and parameter  $D$  is the non-Darcy flow factor,

$$D = \frac{\beta \cdot \rho_{sc} \cdot K}{2\pi h r_w \mu_{R, rw}} \dots\dots\dots (5)$$

where  $\rho_{sc}$  is the gas density at standard condition, and the coefficient  $\beta$  ( $ft^{-1}$ ) has been correlated by Firoozabadi and Katz<sup>11</sup> as

$$\beta = f \frac{2.235 \cdot 10^{10}}{(K \cdot krg)^{1.201}} \dots\dots\dots (6)$$

In Equation (6),  $f$  is an adjustable parameter introduced by Coats<sup>12</sup> to reflect uncertainty of the correlation for  $\beta$ .

Thus, with the pseudo-pressure function determined from the pseudo-steady-state model, the quadratic equation (4) can be solved for  $q_g$  for the case with non-Darcy effect.

### Interpretation of One-D Mechanism and GOR Behavior

In field production test, the production GOR data are normally reported. An increasing trend of GOR would signal declining efficiency of a producing condensate well. The production GOR, in addition, is also an essential input requirement to the pseudo-steady-state model. The production GOR data were thus considered a key matching parameter when validating the compositional model (see **Figures 3 and 4**).

We now use the one-D compositional model to analyze the phase behavior, the evolution of the pseudo-steady-state flow regions and the factors governing GOR increase during production. These subjects are important for using the pseudo-steady-state model. Throughout the discussion in this section, the model parameters for Well A (**Table 1**) are used.

**Figure 6** shows the production GOR versus cumulative gas production (CGP). Also plotted are the evolutions of Region 1 and Region 2 during production. We can observe that appearance of Regions 1 and 2 occurs earlier than the increase of GOR from its original value. This implies that during production there is a time period in which the three flow regions co-exist while flow is subject to infinitely-acting-reservoir condition. However, for the case studied, such a flow period is relatively short in the production life. The GOR soon increases and the Region 2 and 1 expand very rapidly (see slopes of Regions 1 and 2 curves in **Figure 6**). Two-flowing-hydrocarbon phases prevailed throughout the entire reservoir after about 10 BSCF CGP according to the model.

**Figure 7** plots the radial pressure profiles versus radial distance from well for several time steps (CGP). It is shown that for  $P(r) > P_{dew}$ , we have a single-phase flow condition. Under such condition, the reservoir pressure is proportional to  $q_g B_g \mu_g \ln(r) / KH$ . Thus, as gas rate,  $q_g$ , declines with time, the slope of pressure in the single-phase regime decreases. This causes the single-phase pressure curves to flatten out faster with time, accelerating the rapid expansion Region 2.

**Figure 8** plots the in-situ condensate saturation versus the grid pressure for several time steps. Both  $S_o$  and pressure being thermodynamic variables, a graphical presentation of these two variables would have bearing on the pseudo-steady-state behavior discussed in the preceding section. From **Figure 8**, we observe that at early times (say  $CGP < 6.5$  BSCF), there is a sharp discontinuity of  $S_o$  curves changing from zero

to a value of about 32% PV (the critical condensate saturation). This numerical result confirms the steady-state infinitely-acting reservoir flow condition discussed in the preceding section. Region 2 is absent and, with  $P_{bh} < P_{dew}$  (see **Figure 7**), Region has appeared during this time period.

A careful study of the  $S_o$  curves in **Figure 8** reveals that at around  $CGP=6.5$  BSCF, (re)vaporization occurs. The timing of (re)vaporization was found to coincide with GOR increase (shown in **Figure 6**). This above observation leads us to investigate closely the causes of GOR increase through phase behavior.

In **Figures 9 and 10**, we plot, respectively, the trends of near well pressure and condensate saturation versus time along with the GOR. **Figure 9** shows that at the time of GOR increase both the bottomhole and near well pressures have already been declining without a particular behavior to explain the GOR increase. **Figure 10** plots the near-well condensate saturation and GOR trends versus CGP. We can see clearly that the GOR increase coincide with the reduction (or re-vaporization) of oil (condensate) saturation.

Thus, the reservoir phase behavior (in-situ condensate re-vaporization) is shown to link directly with the GOR increase. The re-vaporization, in turn, is a result of local fluid composition and pressure. During production of condensate wells, it has been found from compositional simulation<sup>13</sup> and from well testing (e.g. in build-up test of condensate wells) that the in-situ fluid phase behavior, particularly that near the well, may change from a retrograde condensate to a bubble-point behavior. A bubble-point fluid system would release lean solution gas upon pressure decline, bringing about a sharper GOR increase, than would be a retrograde condensate fluid system. **Figure 11** plots the in-situ oil saturation (*in Fr. HCPV*) versus pressure and time based on the compositions of the grid-block 2feet from the wellbore. It is shown that at early time the fluid exhibits a near critical condensate phase behavior. It quickly switches to a near-critical volatile oil behavior at 5.5 BSCF CGP. The trajectory of saturation-pressure for the fluid in the grid-block is also plotted along with the saturation-pressure curves in **Figure 11**. It can be seen from **Figure 11** that at the time of re-vaporization (where  $S_o$  is a maximum in the trajectory) the fluid is a volatile non-critical oil, and with an oil saturation is about 45% HCPV. When pressure further declines, the volatility of fluid gradually reduces, indicated by the milder  $S_o$ -versus-pressure curves in **Figure 11**. The oil saturation near the well remains near 42% HCPV at  $P=3000$  psia. The hydrocarbon components vaporized during the re-vaporization process composed largely of methane-ethane (78 % according to the model). Such vaporized lean gas contributes to sharp increase of GOR and reduces liquid production rate when pressure further declines. The re-vaporization occurs first to fluid closest to the well. It then propagates into the reservoir, thus widening the two-phase region inside the reservoir (see the rapid expansion of Regions 2 and 1 shown in **Figure 6**).

In **Figures 11 and 12**, we demonstrate through model results that significant amount of oil will be left behind a pres-

sure depletion process and that the re-vaporization releases lean hydrocarbons. Such observations argue for early start of pressure maintenance through lean gas injection. The gas injection project in fact has been underway in the Cupiagua field.

### Validating Pseudo Steady State Model for Long Term Deliverability Prediction

One objective of this work is to establish the applicability of pseudo-steady-state model for forecasting long-term well deliverability. The approach taken is to compare the in-situ fluid PVT properties and phase behavior predicted by both pseudo-steady-state and compositional models.

There have published papers which presented results of pseudo-steady-state model versus compositional and black-oil models. Of most relevance to this work are those by Fussell<sup>4</sup> and by Fevang and Whitson<sup>6</sup>. Fussell compared the true steady-state (infinite-acting-reservoir) condensate saturation profile with those from an EOS compositional model for three gas systems. The comparison is thus only valid when the condition of infinite-acting reservoir applies (referring to Prediction C in Fussell's paper). Fevang and Whitson emphasized the important requirement of production GOR which determines the flowing hydrocarbon composition at any time during depletion. The above authors then validated the pseudo-steady-state model for extended production times through comparison of its predicted gas rate versus that by a black-oil model.

In our work, we use directly the EOS compositional model (which was calibrated by the field production data) to establish the validity of the pseudo-steady-state model, particularly for conditions when GOR becomes significantly higher than the original value (namely when two phase flow dominates the entire reservoir).

To validate the pseudo-state-model for wide-ranging production time periods, it is most relevant to examine and compare the in-situ flowing compositions of the compositional model with that recombined from the production GOR (for the pseudo-steady-state model) at the same time step. The flowing compositions in Region 1 were extracted from the compositional model for several time steps of interest. We have found that the extracted flowing compositions versus radial locations at a given time step show striking similarity among themselves, even when production GOR is significantly higher than the original value. **Table 3** lists flowing compositions for two time steps: one with a small Region 1 (at 36.54 Days) and one with Region 1 occupying the entire reservoir (at 300 Days). It is demonstrated that while the reservoir pressure is on steady decline and with increasing production GOR, the in-situ flowing fluid compositions at a time snapshot across the reservoir do confirm closely to a pseudo-steady-state condition.

We then use the production GOR-combined compositions (as shown in **Table 3**) and perform EOS CCE simulations for four selected time steps. The calculated oil saturations are compared with the flowing oil saturations from the compositional model at the grid-block pressures. Similarly, the in-situ oil viscosities are compared. The comparisons are presented in

**Figures 13 and 14**, respectively. For practical purpose, the pseudo-steady-state model can reproduce in-situ phase behavior and PVT properties of a dynamic compositional process, *if values of the producing GOR and boundary pressures are given*. It is interesting to note that the viscosity curve at Time = 300 Days behaves differently from the others, caused by a quite different flowing composition (as shown in **Table 3**).

In **Figure 15**, we compare the gas viscosity calculated by the pseudo-steady-state model with those from the compositional model in Regions 3 and 2 for several applicable time steps. The pseudo-steady-state results were generated by performing an EOS CVD, as first suggested by Fevang and Whitson<sup>6</sup>, using the original composition.

### Pseudo-Steady-State Model Prediction of Gas Rates

In the preceding section, we have demonstrated that, given a production GOR, the pseudo-steady-state theory model can predict practically the same in-situ fluid PVT properties and phase behavior as those from a much complicated compositional model. This establishes the applicability of using pseudo-steady-state model to calculate well deliverability (or gas production rate), given the parameters (production GOR, Pbh and Pr).

A pseudo-steady-state model was developed via an Excel spreadsheet calculation. The model was then tested using the gas production data from Well B (of **Table 1**) for four flowing bottomhole pressures. The corresponding producing GORs are also available from well separator tests.

In the Excel spreadsheet calculation, the parameter regression option was utilized. Thus, certain model parameters (e.g. Skin, or KH value determined from well testing) can be calibrated to match field measured rates. In our work, the well-test reported skin ( $S=10$ , Well B in **Table 1**) was adjusted to a value of 12.25. Such a slight alteration of skin parameter may improve the compositional model parameter. Recall that in our compositional model results (see **Figure 3**), the cumulative gas produced (CGP) was adopted as the independent variable. CGP, being an independent variable, could mask different model results (e.g. production GOR) caused by a slight difference in model parameters (e.g. value of skin used).

In **Figure 16** the model-calculated rates are compared with the field data. It is shown that an excellent match can be achieved with the pseudo-steady-state model.

### Conclusion

1. A one-D compositional model was developed to simulate production of three condensate wells from the giant near-critical condensate Cupiagua field in Colombia. The characteristics of the production behavior, in terms of production GOR versus cumulative gas production and a pressure-buildup test, are accurately matched by the compositional model. Apart from appropriate input data for the rock and for the fluid (through EOS), the key parameters affecting the production behavior among the three wells are the degree of fluid undersaturation and the drainage radius

associated with each well.

2. The pseudo-steady-state formulation was analyzed. It was shown that during the early stable-flow (or infinitely-acting-reservoir) period, a flow region, containing a flowing gas and an immobile condensate liquid or Region 2, cannot exist. As a result, during such condition, the condensate saturation exhibits a sharp discontinuity from zero to the critical condensate saturation when the local reservoir pressure drops below the original dew point pressure. Such a behavior was verified through the numerical compositional model.
3. The production GOR is a crucial parameter for assessing the producing efficiency and as an input to the pseudo-steady state model. Through compositional model results, we show that the GOR increase is directly related to the revaporization of the oil near the producing well. In particular, at the time of revaporization, the near wellbore fluid has changed to a bubble-point system from an original near critical condensate system. The relatively lean solution gas released during pressure depletion contributes to the significant GOR increase after revaporization occurs.
4. The in-situ flowing compositions from the compositional model were extracted and compared with the composition calculated from the production GOR for several time periods. The very close comparison of these two compositional sets supports the validity of the pseudo-steady-state model, for conditions where the production becomes higher than the original value. Finally, based on field data, we demonstrate that a stand-alone spreadsheet-driven pseudo-steady-state model can be used to calculate accurately the gas production rate, provided that the field production GOR is known.

### Acknowledgments

We gratefully acknowledge BP Exploration and Cupiagua Partners (ECOPETROL, TOTAL and TRITON) for support and permission to publish the work. We thank members of Cupiagua Team in BPX and Partners for stimulating discussions and insights, among them: Jeff App, James Dupree, Doug Handyside, Roberto Ordonez, John Peak, Francis Sommer of BPX, S. Sakthi Kumar and Salvatore Zammito of TOTAL.

### Nomenclature

- $A$  = coefficient defined with Equation (1)  
 $CGP$  = cumulative gas produced, BSCF  
 $D$  = non-Darcy flow factor, Equation (5)  
 $f$  = adjustable parameter for non-Darcy flow in Equation (6)  
 $FBHP$  = flowing bottomhole pressure, psia  
 $GOR$  = gas oil ratio, scf/stb  
 $H$  = reservoir thickness, ft  
 $K$  = absolute permeability, md  
 $kr$  = relative permeability

$K_v/K_h$  = vertical-vs-horizontal permeability  
 $m(P)$  = pseudo-pressure function, Equation (2)  
 $M$  = fluid molecular weight  
 $P$  = pressure, psia  
 $P_r$  = average reservoir pressure, psia  
 $P^*$  = dew point pressure of produced fluid ( $z_i^*$ ), psia  
 $P_{dew}$  = dew point pressure of original fluid, psia  
 $q_g$  = volumetric gas production rate, mmscf/day  
 $r$  = radius, ft  
 $S$  = skin  
 $S_o, S_g$  = oil and gas phase saturations  
 $S_{cc}$  = critical condensate saturation  
 $T$  = temperature  
 $x_i$  = component mole fraction in oil (condensate) phase  
 $y_i$  = component mole fraction in gas phase  
 $z_i$  = referring to overall component mole fraction in the flowing stream  
 $z_i^*$  = the overall composition recombined from production GOR  
 $\beta$  = a coefficient for non Darcy flow, ft<sup>-1</sup>, Equation (6)  
 $\beta_s$  = surface gas mole fraction in produced stream  
 $\mu$  = viscosity, cp  
 $\rho$  = density, gm/cc

### Subscripts

$bh$  = bottomhole condition  
 $e$  = reservoir drainage radius  
 $g$  = gas  
 $i$  = fluid component index  
 $s$  = surface condition  
 $w$  = wellbore condition

### References

1. Kalaydjian, F. J.-M., Bourbiaux, B.J., and Lombard, J.-M., "Predicting Gas Condensate Reservoir Performance: How Flow Parameter are Altered when Approaching Production Wells," paper SPE 36715 presented at the 1996 SPE Annual Technical Conference and Exhibition, Denver, CO, 6-9 October.
2. Boom, W., Wit, K., Schulte, A.M., Oedai, S., Zeelenberg, J.P.W., and Maas, J.G., "Experimental Evidence for Improved Condensate Mobility at Near-wellbore Flow Conditions," paper SPE 30766 presented at the 1995 SPE Annual Technical Conference and Exhibition, Dallas, TX, 22-25 October.
3. O'Dell, H.G. and Miller, R.N., "Successfully Cycling a Low Permeability, High Yield Gas Condensate Reservoir," JPT (January 1967), 41; Trans. AIME, 240.
4. Fusell, D.D., "Single-Well Performance Predictions for Gas Condensate Reservoirs," JPT (July 1973) 256; Trans. AIME, 255.
5. Jones, J.R. and Raghavan, R., "Interpretation of Flowing Well Responses in Gas Condensate Wells," paper 14204 presented at the 1985 SPE Annual Technical Conference and Exhibition, Las Vegas, Nevada, 22-25 September.
6. Fevang, O. and Whitson, C. H., "Modeling Gas-Condensate Well Deliverability," SPERE (November 1996) 221.
7. Personal communication with C.H. Whitson, December 1995; also Belery, P. and da Silva, F.V., "Gravity and Thermal Diffusion in Hydrocarbon Reservoir," paper presented at the 3rd Chalk Research Program, Copenhagen, June 1990.
8. Fluid Analysis, West Port Laboratory, Houston, TX (1996)
9. Gondouin, M., Iffly, R. and Husson, J. "An Attempt to Predict the Time Dependence of Well Deliverability in Gas Condensate Fields," SPEJ (June 1967) 112; Trans. AIME, 240.
10. Kniazeff, V.J. and Naville, S.A., "Two-Phase Transient Radial Flow," SPEJ (June 1967) 125.
11. Firoozabadi, A., and Katz, D.L., "An Analysis of High Velocity Gas Flow Through Porous Media," JPT (Feb. 1979), 211.
12. Coats, K.H., Thomas, L.K., and Pierson, R.G., "Compositional and Black Oil Reservoir Simulation," SPE 29111, 1995.
13. Novosad, Z., "Composition and Phase Changes in Testing and Producing Retrograde Gas Wells," SPERE (November 1996) 231.
14. App, J., "Cupiagua DST and Production Test Report," BPX Internal Document, November 1995.

**Table 1—Base Case Model Input Parameters**

Well	KH (ft-md)	Skin	Turbulence (mscf/d) <sup>-1</sup>	Kv/Kh	Porosity
A	9000	0	6.4x10 <sup>-5</sup>	0.1	0.06
B	3540	10	6.4x10 <sup>-5</sup>	0.1	0.06
C	2352	10	0	0.1	0.06

**Table 2—Reservoir Fluid Parameters**

Well	Original Reservoir P & T		Original Dew Point	Degree of Undersaturation
	T(°F)	P (psia)	P (psia)	ΔP (psia)
A	298	6700	5311	1389
B	267	6005	5338	667
C	245	5980	5354	626

**Table 3—GOR-Recombined Composition and In-Situ Model Flowing Compositions**

Simulation Time (days)	Components	Composition from GOR	Flowing Compositions from Compositional Model			
			Minimum	Mean	Maximum	Standard Deviation
36.54	CO2	0.03243	0.03243	0.03243	0.03243	7.325E-07
	C1N2	0.61416	0.61415	0.61423	0.61425	2.548E-05
	C2	0.09975	0.09975	0.09975	0.09975	2.045E-06
	C3-4	0.09120	0.09120	0.09120	0.09120	1.514E-06
	C5-6	0.03629	0.03628	0.03628	0.03629	1.974E-06
	C7-10	0.06344	0.06341	0.06342	0.06344	8.214E-06
	C11-14	0.02466	0.02464	0.02465	0.02466	3.447E-06
	C15-20	0.01888	0.01886	0.01887	0.01888	3.507E-06
	C21-29	0.01329	0.01327	0.01327	0.01329	4.909E-06
C30+	0.00591	0.00590	0.00590	0.00591	3.421E-06	
300	CO2	0.03404	0.03403	0.03404	0.03404	2.344E-06
	C1N2	0.67377	0.67364	0.67377	0.67384	3.594E-05
	C2	0.10231	0.10230	0.10231	0.10232	2.776E-06
	C3-4	0.08711	0.08711	0.08711	0.08714	6.393E-06
	C5-6	0.03093	0.03092	0.03093	0.03097	8.714E-06
	C7-10	0.04219	0.04216	0.04220	0.04232	3.010E-05
	C11-14	0.01584	0.01582	0.01584	0.01590	1.409E-05
	C15-20	0.00965	0.00964	0.00965	0.00971	1.298E-05
	C21-29	0.00335	0.00328	0.00334	0.00336	1.800E-05
C30+	0.00081	0.00072	0.00080	0.00081	2.053E-05	

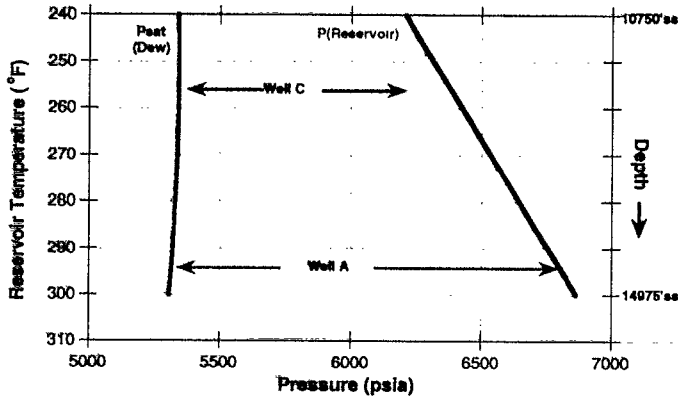


Figure 1—Cupiagua Temperature (Depth) Pressure Behavior

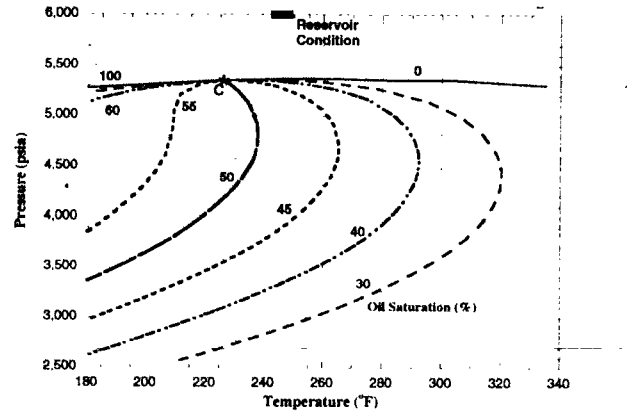


Figure 2—Cupiagua Well Sample Pressure-Temperature Phase Diagram

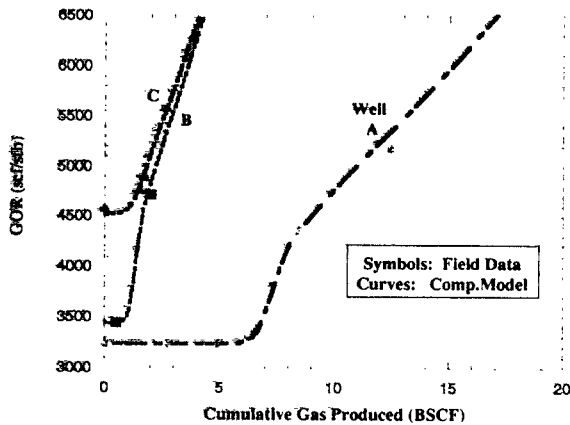


Figure 3—Model Calculated GOR versus Cumulative Gas Production Wells: A, B and C

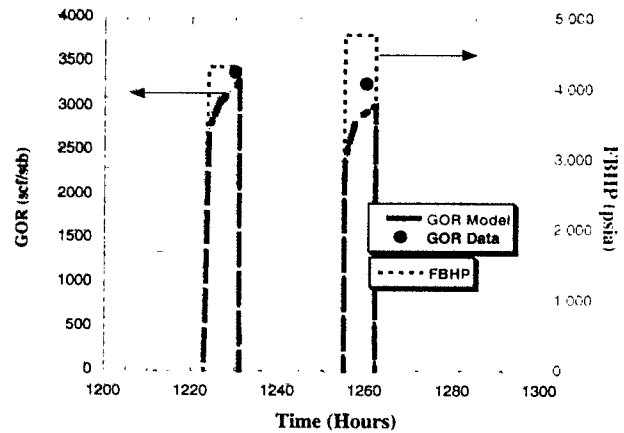


Figure 4—Pressure Buildup Test of Well B: Model Simulation versus Data

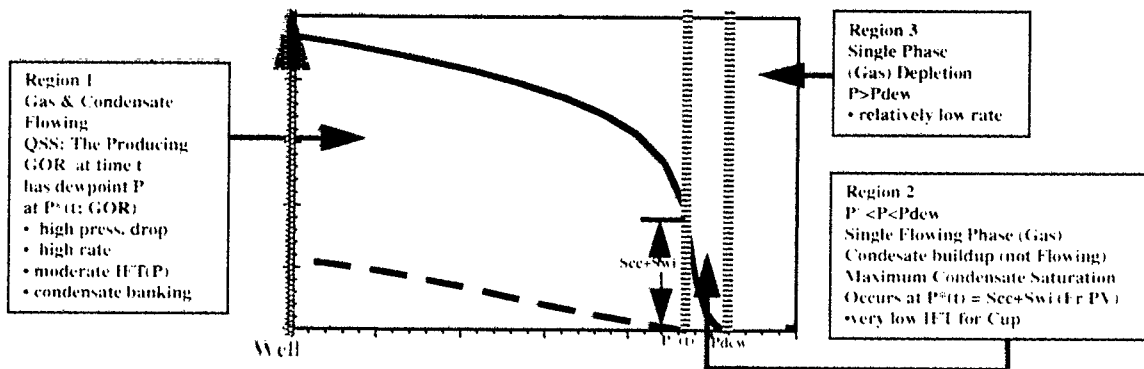


Figure 5—Schematics of 3 Flow Regions in Depleting Condensate Reservoir

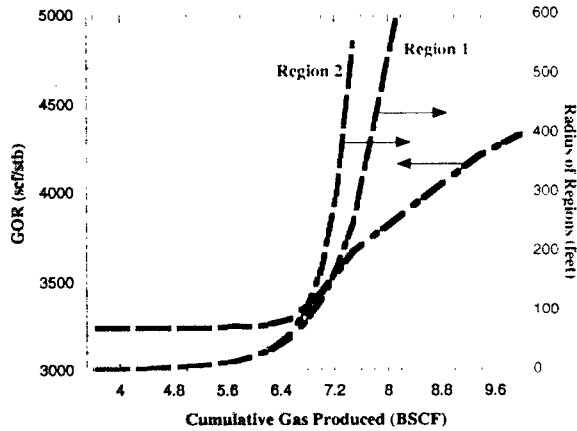


Figure 6—Regions 1 (FBHP<P<P\*) and Region 2 (P\*<P<Pdew) Growth and GOR Behavior (Well A)

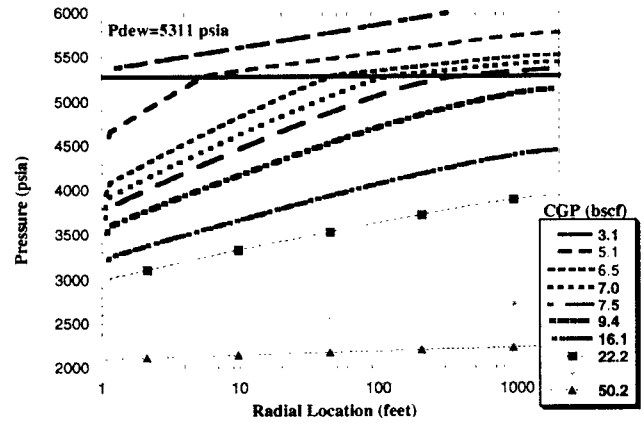


Figure 7—In-Situ Radial Pressures for Different Cum Gas Production

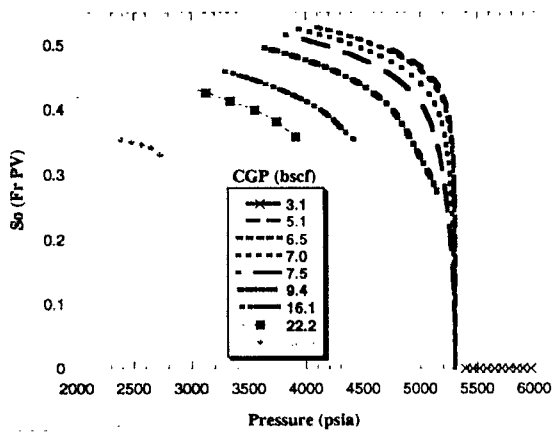


Figure 8—In-Situ Condensate Banking and Revaporization

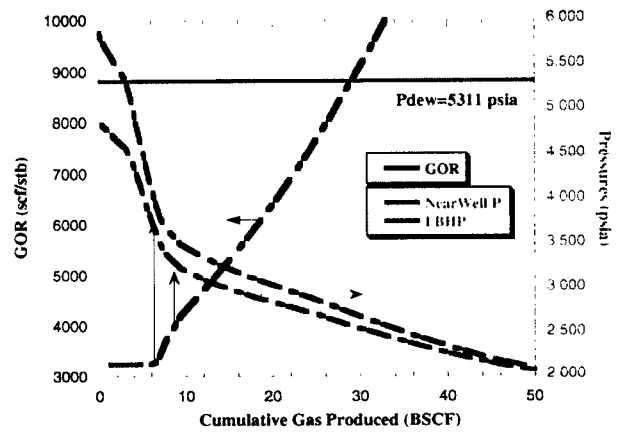


Figure 9—Production GOR behavior versus Near Well Block Pressure (Well A: THP=1200 psia)

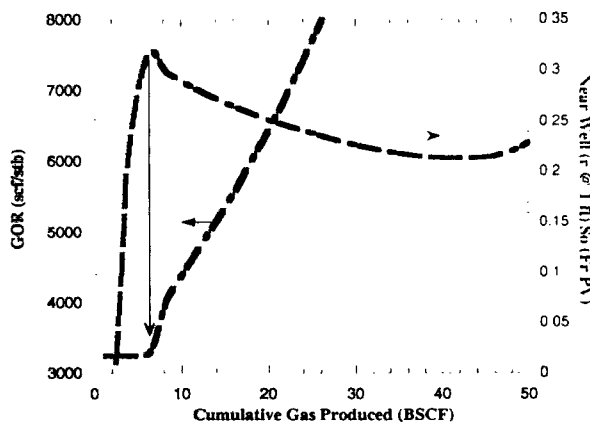


Figure 10—Production GOR & Near Well Condensate Saturation versus Cumulative Gas Production (Well A)

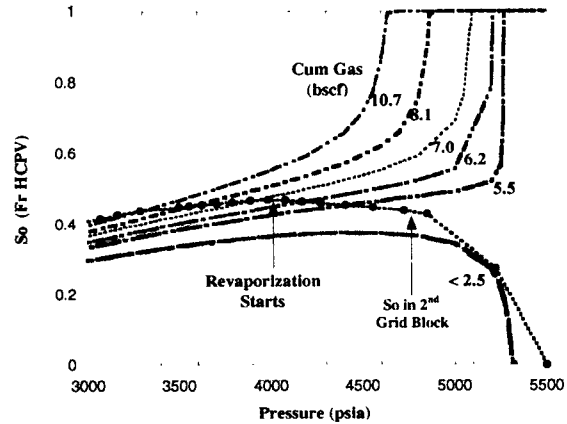


Figure 11—Near Well (r @ 2ft) Fluid Phase Behavior and Flow Mechanism

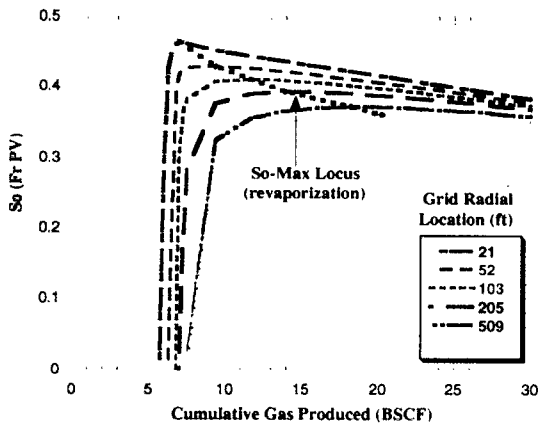


Figure 12—Oil Saturations at Radial Locations versus Time Revaporization Trend

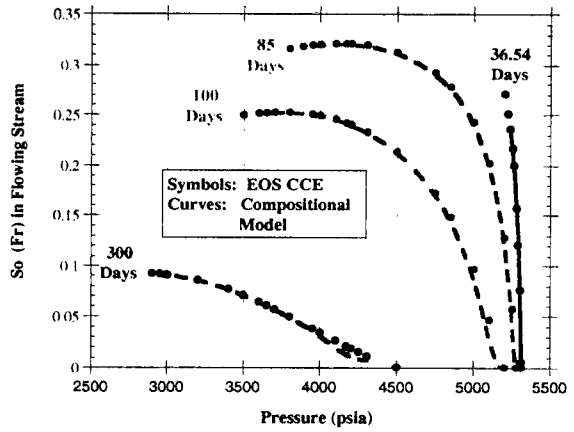


Figure 13—Pseudo S.S. Theory: EOS CCE and VIP-Calculated Flowing Condensate Saturation (Well A)

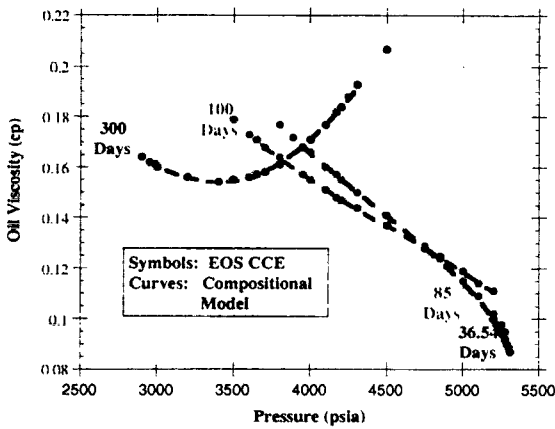


Figure 14—Pseudo S.S. Region 1: EOS CCE and VIP-Calculated Oil Viscosity (Well A)

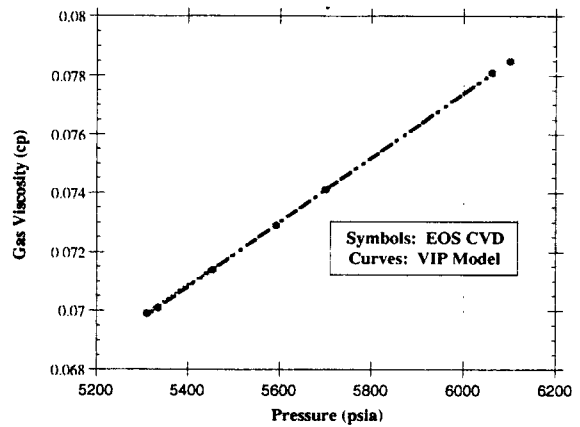


Figure 15—Pseudo S.S. Region 3&2: EOS CVD and VIP-Calculated Gas Viscosity (Well A)

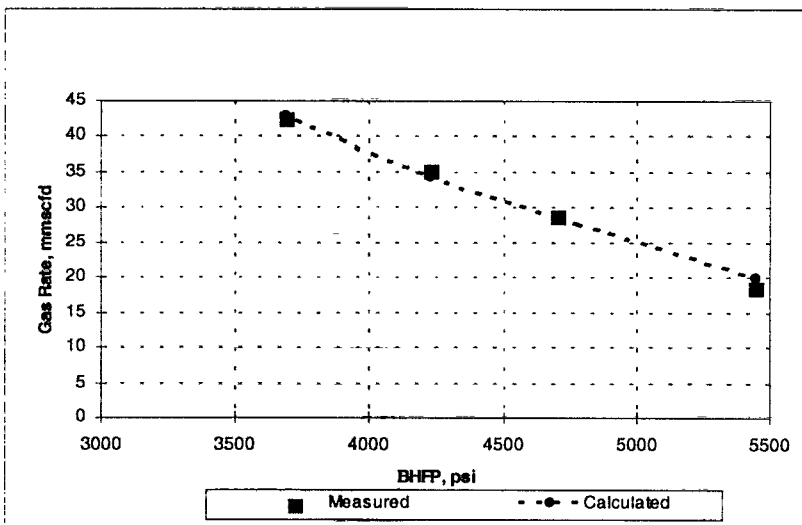


Figure 16—Comparison between Measured and Calculated Gas Rates